Int. J. Electrochem. Sci., 8 **(2013)** 12367 - 12376

International Journal of
ELECTROCHEMICAL
SCIENCE
www.electrochemsci.org

Effects of Synthesis Conditions on the Structural and Electrochemical Properties of the Li-doped Material $Li_{1+x}(Ni_{0.5}Mn_{0.5})_{1-x}O_2$(x=0.05) Via a Carbonate Co-precipitation Method

Song Teng-fei, Zhang Hai-lang[*]

School of Chemical and Material Engineering, Jiangnan University, Wuxi ,Jiangsu 214122,China
[*]E-mail: zhl8868@vip.163.com

Received: 12 July 2013 / *Accepted:* 18 August 2013 / *Published:* 25 September 2013

The Li-doped layered cathode material $Li_{1.05}(Ni_{0.5}Mn_{0.5})_{0.95}O_2$ with ball-like shape was successfully synthesized by carbonate co-precipitation method, followed by a calcination process at different temperatures. The effects of calcination temperature on the crystal structure, morphology and electrochemical performance were investigated by employing X-ray diffraction(XRD), scanning electromicroscopy(SEM) and galvanostatic charge/discharge tests. It is found that the sample S(850-950) prepared by the novel two-stage sintering process has the best electrochemical performance among the prepared materials, especially its rate capability is excellent. An initial discharge capacity of 190.8mAhg^{-1} and 136.8mAhg^{-1} at 0.1C and 1C was obtained between 2.5-4.5V, respectively. The excellent electrochemical performance is attributed to the good order structure, moderate crystallinity and short diffusion distance.

Keywords: Li-ion battery; cathode material; Carbonate co-precipitation; two-stage sintering process; electrochemical performance

1. INTRODUCTION

Lithium-ion batteries have been widely used as power sources for various electronic devices, such as cell phones, laptop computers and digital cameras, etc and have long been considered as possible power source for HEVs and EVs due to their light weight, high power density and long cycle life [1]. Currently, $LiCoO_2$ is the predominant cathode material for lithium-ion batteries because of its easy preparation and excellent cycling performance [2]. However, the relatively high cost and high toxicity of cobalt and low practical capacity have led to the evaluation of other possible cathode

materials that offer low cost, high energy density, longer life, and improved abuse tolerance [3-5]. Manganese-based lithium metal oxides are promising electrode materials.

Among those electrode materials, $Li(Ni_{0.5}Mn_{0.5})O_2$ is particularly attractive due to its higher specific capacity ,good cycling performance and excellent thermal stability, as well as lower cost and toxicity due to the absence of cobalt [6,7]. Unfortunately, to synthesis battery-active $Li(Ni_{0.5}Mn_{0.5})O_2$ is difficult by traditional methods because of the existing of 8%-10% Li-Ni exchange due to their similar ionic radii Ni^{2+}(0.069nm)and Li^{+}(0.076nm) [8,9]. The cation mixing between lithium and nickel ions will blocks the pathway of lithium diffusion, and then deteriorate the electrochemical performance [10,11].

Some strategies have been proposed to overcome this issue. One effective method is the adopting of co-precipitation synthetic method which can lead to homogenous cation distribution and the possibility of controlling size and morphology of the particles. The hydroxide co-precipitation method is one of the powerful methods. However, $Mn(OH)_2$ in nickel manganese double hydroxides is easily oxidized to Mn^{3+}(MnOOH) or Mn^{4+}(MnO2), which may lead some impurity in $Li(Ni_{0.5}Mn_{0.5})O_2$, which can severely deteriorate the electrochemical properties [12]. The carbonate co-precipitation method is a very effective method, due to the stability of the $MnCO_3$ precursor under ambient atmosphere, which is markedly different from the hydroxide co-precipitation method curried out under Ar or N_2 [13].

Another effective method is cation substitution for transition metal. If some Mn and Ni cations are substituted for lithium, then Li-excess $Li_{1+x}(Ni_{0.5}Mn_{0.5})_{1-x}O_2$ materials are formed resulting in less site disorder, and improved electrochemical performance [14-16]. Besides, Li has the smallest atomic weight and such substitution results in limited decrease in specific capacity. Furthermore, the extra capacity result from the relative excess lithium delivered at about 4.5V can be very attractive for high-energy lithium-ion batteries [17].

In this work, with an aim of achieving a high-performance cathode material, we have combined the advantages of the two strategies mentioned above.

2. EXPERIMENTAL

2.1. Material preparation

Spherical $(Ni_{0.5}Mn_{0.5})CO_3$ precursor was synthesized by carbonate co-precipitation method. An aqueous solution was prepared by dissolving the salts of $Ni(OAc)_2{\cdot}4H_2O$(AR) and $Mn(OAc)_2{\cdot}4H_2O$ (AR)(mole ratio 1:1) in distilled water with a concentration of 2mol/L and then pumped into the reactor. At the same time, Na_2CO_3 solution of 2mol/L and desired amount of NH_4HCO_3 were also separately fed into the reactor. The pH(8.0), temperature(60 ^{o}C), and stirring speed of the mixture were carefully controlled. After vigorous stirring for 6h, the spherical $(Ni_{0.5}Mn_{0.5})CO_3$ precursor was filtered and washed completely, and dried in a vacuum at 80 ^{o}C overnight. Then, a 5% excess amount of Li_2CO_3 (excess amount of lithium was used to compensate the portion of lithium evaporation at high temperature) was mixed thoroughly with the precursor using ethanol as medium. The mixture was calcined first at 500 ^{o}C for 6h, and subsequently at various temperatures in air.

2.2. Physical characterization

The thermal decomposition behavior of the precursors was examined by means of the thermogravimetry (TG). X-ray diffraction (XRD, Bruker D8 with Cu Kα radiation, λ= 1.5406A˚) was employed to analyze the structure of prepared materials. The diffracted data were collected from 10 ^{o} to 90 ^{o} in 2θ with a step size of 0.02 ^{o}. The scanning electron microscopy (SEM, S4800) images were taken to observe the morphology and size of the materials.

2.3. Electrochemical measurement

The electrochemical characterization were examined using CR2032 coin type half-cell, which contains cathode and Li metal anode separated by a porous polypropylene film(Celgard 2325) and electrolyte consisting 1M $LiPF_6$/EC + DEC(1:1 in volume). The cathode electrodes were prepared by homogeneously mixing active material, acetylene black and PVDF binder in a mass ration of 80:12:8 in N-methyl-2-pyrrodidene (NMP) and then coating the cathode-slurry onto an Al foil , followed by drying at 80 ^{o}C for 24 h. Finally, the cell was assembled in glove box filled with argon. The charge–discharge tests were operated in the voltage range of 2.5–4.5V at the different current density (180 mA/g was assumed to be the 1C rate capacity).

3. RESULTS AND DISCUSSION

3.1 Thermal analysis

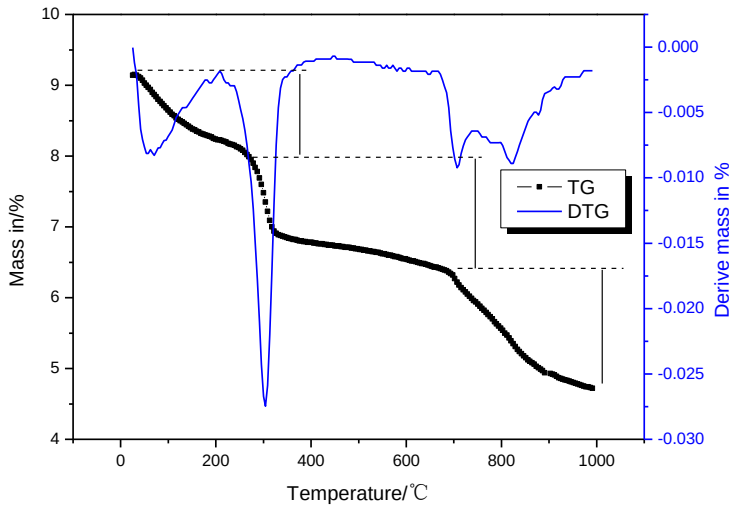

Figure 1. TG/DTG profiles for the carbonate precursor mixed with Li_2CO_3.

Through the carbonate co-precipitation process, green-colored $(Ni_{0.5}Mn_{0.5})CO_3$ precursor was obtained. The TG/DTG profiles for the precursor in the temperature range of 25-1000 ^{o}C is shown in Fig.1 The decomposition process of the mixture is supposed to be divided into three stages. The loss of

weight from room temperature to 220 °C can be assigned to the loss of absorbed water and crystal water. The main weight loss around 300 °C is associated with the decomposition of $(Ni_{0.5}Mn_{0.5})CO_3$. The weight loss above 700 °C is due to the decomposition of Li_2CO_3 and formation of the target product. The decomposition process can be regarded as the following reactions:

$$(Ni_{0.5}Mn_{0.5})CO_3 \cdot 2H_2O \rightarrow (Ni_{0.5}Mn_{0.5})CO_3 + 2H_2O \quad (1)$$

$$2(Ni_{0.5}Mn_{0.5})CO_3 + 1/2O_2 \rightarrow NiMnO_3 + 2CO_2 \quad (2)$$

$$NiMnO_3 + Li_2CO_3 \rightarrow 2LiNi_{0.5}Mn_{0.5}O2 + CO_2 \quad (3)$$

The flowing sintering process is selected according to the TG/DTG result. First the precursor was preheated at 500 °C for 6h, and then between 850 °C and 950 °C for 12h in air. Hereafter, the materials synthesized at 850 °C for 12h, 900 °C for 12h,950 °C for 12h were referred as S(850), S(900), S(950), respectively, and a novel two-step sintering process at 850 °C for 6h and then at 950 °C for 6h is marked as S(850-950).

3.2 Structure and morphology characteristic

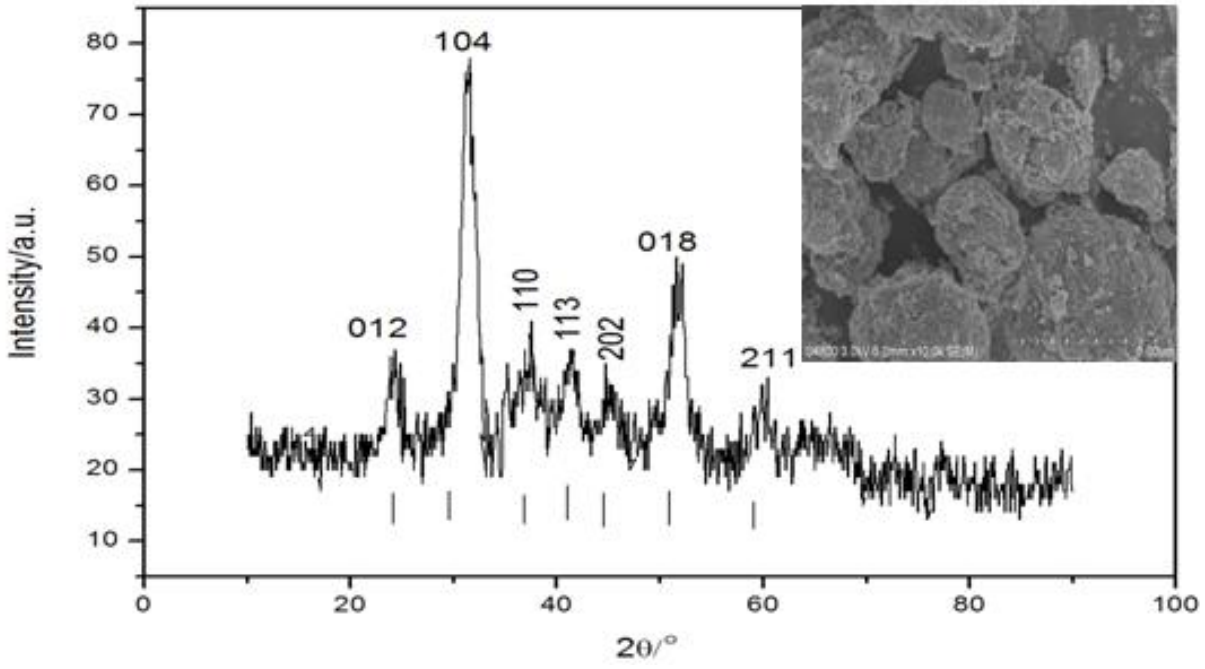

Figure 2. XRD patterns and the SEM images of the $(Ni_{0.5}Mn_{0.5})CO_3$ precursor..

Fig.2 shows the XRD patterns and the SEM images of the $(Ni_{0.5}Mn_{0.5})CO_3$ precursor. All main characteristic peaks were well coincided with ideal $MnCO_3$ patterns(space group R-3C,JCPDS No.44-1472),except for relatively broader integrated peaks which can be attributed to the mixture of $MnCO_3$ and $NiCO_3$[12].The particle morphology of the precursor is spherical with average particle size around 5um，and the whole dispersion performance is well.

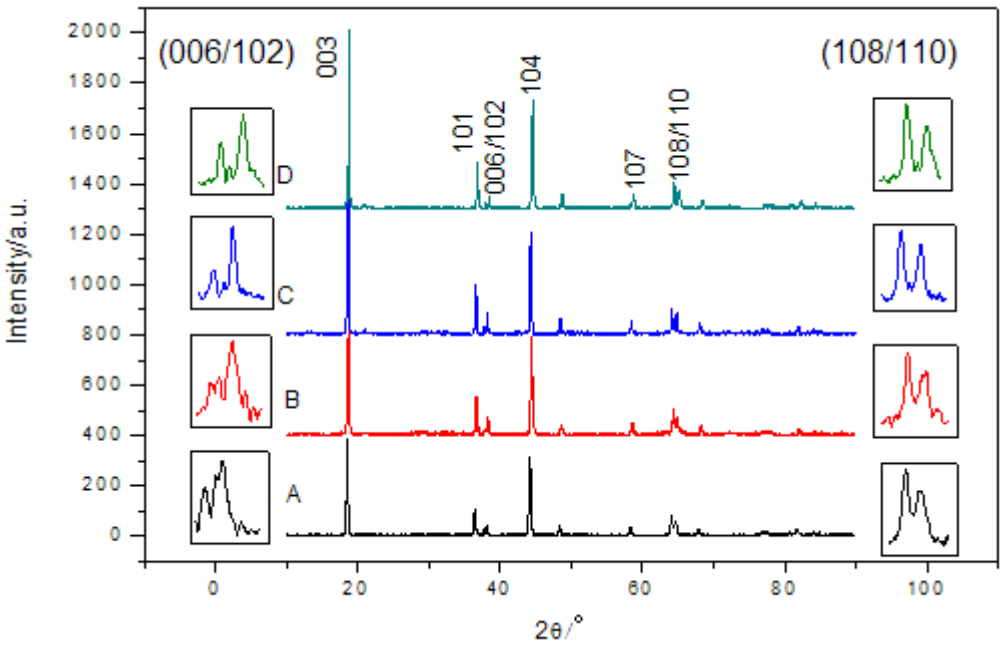

Figure 3. XRD patterns of $Li_{1.05}(Ni_{0.5}Mn_{0.5})_{0.95}O_2$ synthesized at different temperatures.

Table 1. Lattice parameters and electrochemical characteristics of $Li_{1.05}(Ni_{0.5}Mn_{0.5})_{0.95}O_2$ synthesized at different temperatures.

Sample	Crystal parameter				$I_{(003)}/I_{(004)}$	Charge capacity $mAhg^{-1}$	Discharge capacity $mAhg^{-1}$	Coulombic efficiency(%)
	a/nm	c/nm	c/a	v/nm^{-3}				
A	0.2861	1.4211	4.967	102.54	1.31	202.6	176.6	87.18
B	0.2870	1.4258	4.968	102.49	1.40	205.3	180.9	88.11
C	0.2874	1.4292	4.973	102.63	1.44	212.6	192.4	90.50
D	0.2872	1.4294	4.977	102.68	1.52	211.5	190.8	90.21

XRD patterns of all the synthesized $Li_{1.05}(Ni_{0.5}Mn_{0.5})_{0.95}O_2$ at different calcination temperatures are presented in Fig.3. All diffraction peaks of materials can be indexed to a layered hexagonal structure of α-NaFeO2 (space group: R3m). As the calcination temperature increases, the separation of (006)/(102) and (108)/(110) become more clearly, suggesting that the compound synthesized is well crystallized. But when the temperature reached 950 ^oC, small additional peaks at 20–25◦ appeared, which can be attributed to superstructure in hexagonal ABO_2 lattice or to the Li_2MnO_3 [16].The lattice parameters calculated by the software JADE5.0 are listed in Table1. With increasing calcination temperature, calculated lattice parameter were somewhat increased, and sample S(850-950) has the largest *c*/*a* values which indicates a better channel for Li^+ to transfer through[19].

It was reported that the undesirable cation mixing would appear when the ratio of I_{003}/I_{004} is smaller than 1.2[20]. As shown in Fig.1, the I_{003}/I_{004} values of all samples in this work are larger than

1.2, indicating less undesirable Li^+/Ni^{2+} cation mixing exists in the as-prepared samples due to the carbonate co-precipitation process

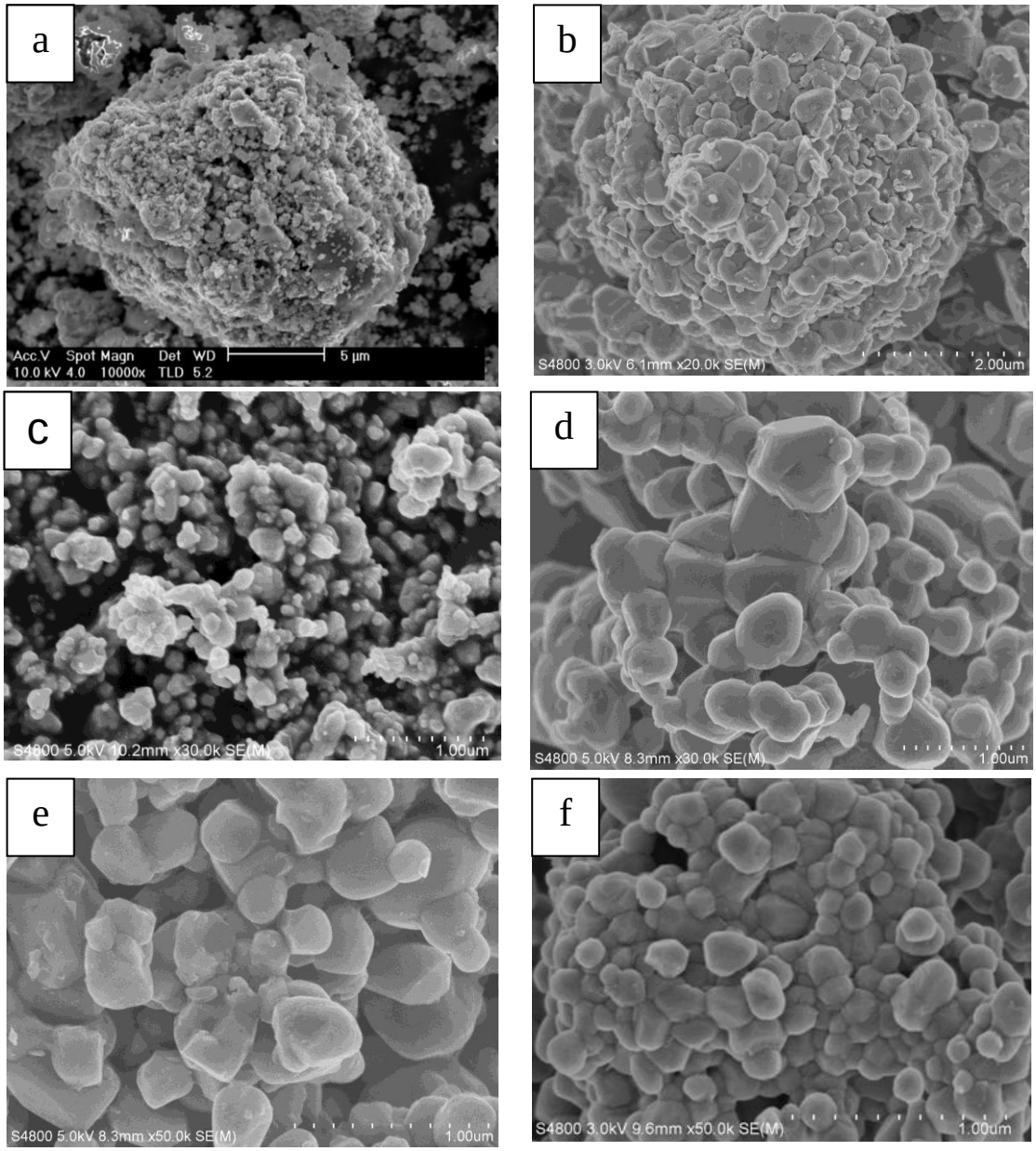

Figure 4. SEM images: (a and c) for S(850) at two magnifications; (b and f) for S(850-950) at two magnification; (d) S(900); (e)S(950).

Scanning electron micrographs(SEM) was applied to observe the morphology change at different calcination temperatures. Fig.4(a) and (b) illustrate that the compound maintains the spherical morphology with the average particle size around 5um after high temperature calcination, which are very similar to precursor power; and each of the spherical particles is comprised of a large number of small primary grains in nanometric. But S(850) is obviously not crystallized well enough, due to the

low temperature. By comparing the samples (c), (d), (e), the primary particles grow bigger with increasing sintering temperature. But the morphology of (e) is somewhat particle-agglomerated and melted together, which is attributed to the high temperature for a long time, and this morphology may lead the electrochemical properties obviously decreased.

It is worth noting that, the morphology of Fig.(g) is smooth, distribution well and stack more closely, which will benefit to improve inter-particle lithium ion movement, thereby enhancing the tap density and rate capability [21].

From the XRD and SEM discussed above, we believe that the novel two-step sintering process is very effective in obtaining the best electrochemical properties.

3.3. Electrochemical properties

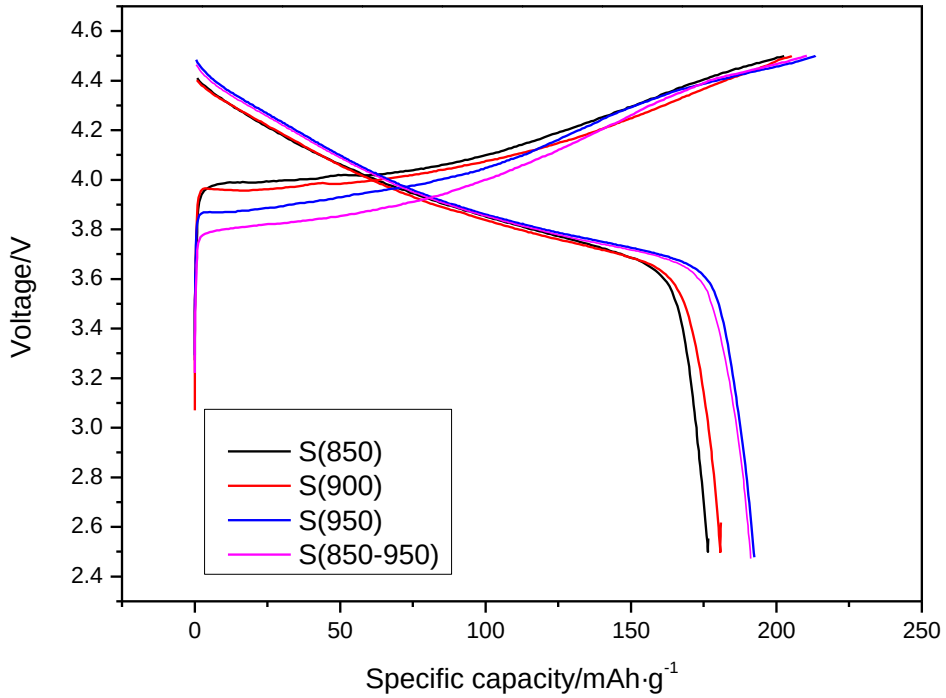

Figure 5. Initial charge-discharge curves of $Li_{1.05}(Ni_{0.5}Mn_{0.5})_{0.95}O_2$ synthesized at different temperatures.

Fig.5 shows the initial charge-discharge curves of $Li_{1.05}(Ni_{0.5}Mn_{0.5})_{0.95}O_2$ at 0.1C between 2.5V and 4.5V. With the increase of synthesis temperature, the initial discharge capacity increases from 176.6mAhg^{-1} to 192.4mAhg^{-1}. S(950) delivers the largest initial discharge capacity, that may be due to the highly crystallinity synthesized at the high temperature. All samples had first irreversible capacity, which may result from the extraction of lithium and oxygen due to the excess lithium as well as the possible of electrolyte decomposition [22]. But the irreversible capacity loss also slightly decreased with increasing calcination temperature.

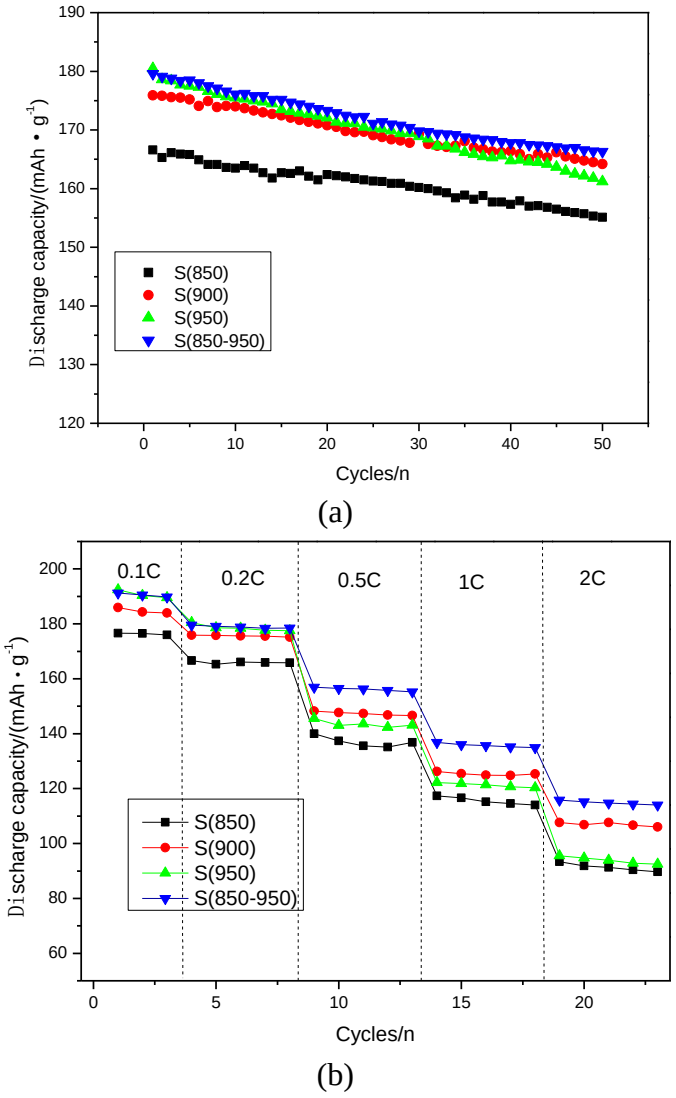

Figure 6. (a)The cycle performance at a discharge rate of 0.2C; (b) Rate capability of $Li_{1.05}(Ni_{0.5}Mn_{0.5})_{0.95}O_2$ synthesized at different temperatures .

To study the effect of calcination temperature on the cycle performance, all samples were tested between 2.5-4.5Vat 0.2C for 50 cycles. As shown in Fig.6 (a), though the sample sintered at 950 ^{o}C delivers the highest initial capacity, it shows a more distinct decrease in capacity, leading to a capacity retentions of only 89.4% after 50cycles, compared with 93.1%, 93.4% and 92.9% for S(850) ,S(900) ,S(850-950), respectively.

Fig.6 (b) compares the rate capability of all samples ranged from 0.1C to 2C-rate between 2.5-4.5V. All samples show decreased capacities at high C rate, but S(900) and S(850-950) exhibit a superior rate capability than S(850) and S(950). For example, S(850-950) provided capacity retentions of 71.6% and 60.5% at the 1C and 2C respectively with respect to that at 0.1C, compared to the corresponding values of 63.5% and 49.6% for S(950). A less better layered structure formed at 850 ^{o}C makes it delivered the lowest capacity at all current rate. But the S(950) also shows the poor cycle and rate capability, which may due to the particle-agglomerated with longer high temperature treatment.

The big agglomerated particles have a relatively smaller active area to the electrolyte and will embarrass the diffusion of Li^+.

Therefore, from above discussion, we can make the conclusion that a appropriate sintering temperature is one of the key factors to obtain the best electrochemical properties.

To sum up, the synthesized $Li_{1.05}(Ni_{0.5}Mn_{0.5})_{0.95}O_2$ by the two-stage sintering process has the best electrochemical performance because of the moderate crystallinity and large surface.

4. CONCLUSION

The Li-doped layered cathode material $Li_{1.05}(Ni_{0.5}Mn_{0.5})_{0.95}O_2$ with ball-like shape has been successfully synthesized by carbonate co-precipitation method under different calcination temperatures. The effects of calcination temperature on the crystal structure, morphology and electrochemical performance are investigated in detail. All the materials show clear splitting of (006)/(102) and (108)/(110) and the particle size grows bigger with the increase of temperature. The sample S(850-950) prepared by the novel two-stage sintering process delivered a high discharge initial capacity of 190.8mAhg^{-1} between 2.5-4.5V, showing the best cycle performance and rate capability. The excellent electrochemical performance is attributed to the moderate crystallinity and large surface.

References

1. J.J. Liu, J. Wang, Y.G. Xia, X.F. Zhou, Y. Saixi,,and Zh.P. Liu, *Materials Research Bulletin*,47(2012)807.
2. P.Mohan , G. P. Kalaignan, *Ionics*, 19,(2013)895.
3. K.Amine, Z.H. Chen, and S.-H. Kang, *J. Fluorine Chem.*,128(2007)263.
4. S.-W. Cho, K.-S. Ryu, *Mater. Chem. and Phys.*,135(2012)533.
5. J.G. Li, Y.Y. Zhang, J.J. Li, Wang L, X.M. He,and J. Gao, *Ionics* 17(2011)671.
6. T. Ohzuku , Y. Makimura,.*Chem.Lett*,30(2001)740.
7. K.-S. Lee, S.-T. Myung, J.-S. Moon, and Y.-K.Sun, *Electrochimica Acta*,53(2008)6033.
8. H.Xia, S.B. Tang,and L.Lu, *J. Alloys and Compounds* ,449 (2008)296.
9. X.L.Meng, S.M.Dou , W.L.Wang, *J.Power Sources*, 184 (2008)489.
10. X.Y. Zhang, W.J. Jiang, A. Mauger, L.Qi, F.Gendron, and C.M. Julien, *J. Power Sources*,195(2010)1292.
11. K.-S. Lee, S.-T. Myung, J. Prakash, H. Yashiro, and Y.-K. Sun, *Electrochim. Acta*,53(2008) 3065.
12. T.H. Cho, S.M. Park, M. Yoshio, T. Hirai, and Y. Hideshima, *J. Power Sources*,142 (2005)306.
13. Y. Wang , N. Sharma, D.W. Su , and D. Bishop , H. Ahn, G.X. Wang, *Solid State Ionics*,233(2013)12.
14. S.-H. Park, S-H.Kang , C.S. Johnson, K. Amine, and M.M. Thackeray, Elec*trochem. Commun.*,9(2007)262.
15. D.H. Kim, S.-H. Kang, M Balasubramanian, and C. S. Johnson, *Electrochem. Commun.*,12(2010)1618.
16. J. M. Kim, N. Kumagai , Y. Kadoma, and H.Yashiro, *J.Power Sources*,174(2007)473.
17. Z.Q. Deng, A.Manthiram, J Phys. Chem. C, 115(2011)7097.
18. C.Pouillerie , L.Croguennec , C.Delmas, *Solid State Ionics*, 132(2000)15.
19. B.J.Hwang , R. Santhanam , C.H.Chen, *J. Power Sources*,114(2003)244.

20. S.Y.Yang, X.Y.Wang , Q.Q.Chen, X.K.Yang, J.J.Li, Q.L.Wei, *J. Solid State Electrochem*, 16(2012)481.
21. Y.H. Xiang, Z.L.Yin, Y.H.Zhang,X.H. Li, *Electrochim. Acta* ,91(2013)214.